Innovation in metallurgical industrial and laboratory equipment, technologies and materials / **Инновации в металлургическом промышленном и лабораторном оборудовании, технологиях и материалах**

UDC 621.74.045:53.09
DOI 10.17073/0368-0797-2024-5-593-603

Original article
Оригинальная статья

Influence of compression modes of waxy powders on stress-strain state of compacts used in precision casting

N. A. Bogdanova ✉, **S. G. Zhilin**

Institute of Metallurgy and Mechanical Engineering of the Khabarovsk Federal Research Center, Far-Eastern Branch of the Russian Academy of Sciences (1 Metallurgov Str., Komsomolsk-on-Amur, Khabarovsk Territory 681005, Russian Federation)

✉ joyful289@inbox.ru

Abstract. The high demands placed on the surface quality and geometric complexity of metal products, structures and parts produced from a wide range of non-ferrous and ferrous alloys determine the demand for investment casting as a method that provides a range of critical products for the needs of aircraft, ship building and mechanical engineering industries. A number of "bottlenecks" in the implementation of investment casting processes include a significant number of technological operations, each of them is accompanied by phenomena of a thermophysical nature that require correction, and it ultimately determines the high cost of casting. The difficulties arise from phenomena such as shrinkage of the pattern material, its thermal expansion during melting from a ceramic mold, which determines penetration of pattern mass into ceramic pores and can affect the appearance of surface defects, the chemical composition and structure of the alloy of future casting. The process of forming a porous surface on wax patterns without shrinkage defects by pressing powders of waxy materials is aimed at eliminating the noted shortcomings, which ensures the required geometry of the compacts and absence of deformation effects on ceramics of the model material at the stage of its melting. Widespread use of the method is hampered by the lack of information about the features of stress control in the compact body determining the magnitude of elastic response of the compacted material, which is an order of magnitude less than thermal shrinkage. The paper presents the results of an experimental study of influence of the compression rate of powder materials on the stress-strain state of pressed wax patterns formed in a closed matrix, as well as on the strength of these compacts.

Keywords: experimental modeling, mechanical engineering processes, investment casting, stress-strain state, pressing, porosity, elastic response, strength

Acknowledgements: The work was performed within the framework of a state assignment of the Khabarovsk Federal Research Center, Far-Eastern Branch of the Russian Academy of Sciences. The authors used photos by Firsov S.V.

For citation: Bogdanova N.A., Zhilin S.G. Influence of compression modes of waxy powders on stress-strain state of compacts used in precision casting. *Izvestiya. Ferrous Metallurgy*. 2024;67(5):593–603. https://doi.org/10.17073/0368-0797-2024-5-593-603

Влияние режимов уплотнения воскообразных порошков на напряженно-деформированное состояние прессовок, применяемых в точном литье

Н. А. Богданова ✉, **С. Г. Жилин**

Институт машиноведения и металлургии Хабаровского Федерального исследовательского центра Дальневосточного отделения РАН (Россия, 681005, Хабаровский край, Комсомольск-на-Амуре, ул. Металлургов, 1)

✉ joyful289@inbox.ru

Аннотация. Высокие требования, предъявляемые к качеству поверхности и сложности геометрии металлоизделий, конструкций и узлов деталей, получаемых из широкой линейки цветных и черных сплавов, определяют востребованность литья по выплавляемым моделям (ЛВМ) как метода, обеспечивающего номенклатуру изделий ответственного назначения для нужд авиа-, судо-, и машиностроения. К ряду «узких» мест в реализации процессов ЛВМ можно отнести значительное число технологических операций, каждая из которых сопровождается явлениями теплофизической природы, требующих коррекции, что в конченом итоге определяет высокую стоимость литья. Сложность представляют такие явления, как усадка модельного материала, его температурное расширение на стадиях выплавления из керамической формы, определяющее проникновение модельной массы в поры керамики и способное повлиять на появление поверхностных дефектов, химический состав и структуру сплава будущей отливки. На устранение отмеченных недостатков направлен процесс

формирования пористой поверхности выплавляемой модели без усадочных дефектов путем прессования порошков воскообразных модельных материалов, что обеспечивает требуемую геометрию прессовок и отсутствие деформационного воздействия на керамику модельного материала на стадии его выплавления. Широкому распространению метода препятствует недостаток сведений об особенностях управления напряжениями в теле прессовки, определяющими величину упругого отклика уплотняемого материала, который на порядок меньше, чем тепловая усадка. В работе представлены результаты экспериментального определения влияния скорости уплотнения порошковых модельных материалов на напряженно-деформированное состояние прессованных выплавляемых моделей, формируемых в закрытой матрице, а также на прочность таких прессовок.

Ключевые слова: экспериментальное моделирование, машиностроительные процессы, литье по выплавляемым моделям, напряженно-деформированное состояние, прессовка, пористость, упругий отклик, прочность

Благодарности: Работа выполнена в рамках государственного задания Института машиноведения и металлургии Хабаровского Федерального исследовательского центра ДВО РАН. В работе использованы фото Фирсова С.В.

Для цитирования: Богданова Н.А., Жилин С.Г. Влияние режимов уплотнения воскообразных порошков на напряженно-деформированное состояние прессовок, применяемых в точном литье. *Известия вузов. Черная металлургия*. 2024;67(5):593–603. https://doi.org/10.17073/0368-0797-2024-5-593-603

Introduction

A key feature of modern industrial enterprises specializing in the production of products for the automotive, aircraft, and shipbuilding industries is the high demand for metals and the increased production of high-quality cast products with the required set of characteristics, driven by the use of energy- and material-efficient technologies [1 – 4].

In these sectors, it is crucial to reduce costs at all stages of the technological cycle, especially in the formation of castings for high-precision and complex-shaped parts made from a wide range of alloys [5].

One of the most in-demand methods for obtaining precision cast blanks from a variety of structural steels and alloys is investment casting (IC), which allows the creation of complex-shaped products by combining separate parts into all-cast assemblies [6; 7]. The versatility of this method makes it suitable for producing both thin-walled castings of relatively small mass and cast products with linear dimensions of up to 500 mm [8 – 10].

The surface of such castings can achieve a roughness of up to R_a = 1.25 μm, meet quality grades 11 – 16, and achieve mold cavity dimensional tolerances of no more than grades 8 – 9 according to GOST 25347–82 “Basic norms of interchangeability. Unified system of tolerances and fits. Tolerance fields and recommended fits”.

Like any technological sequence, IC has its drawbacks, largely due to the large number of operations involved, which are characterized by a certain degree of irreparable defects. These factors ultimately increase the cost of the final product and complicate the calculation and modeling of the IC process outcomes [11].

The most widely used sequence in IC processes includes the following operations [12]:

– manufacturing of wax models and elements of the gating and feeding systems by injection of the model composition (melt or paste) into the corresponding mold, followed by the assembly of all elements into model clusters;

– layer-by-layer application of ceramic coating to the model cluster and drying of the ceramic shell;

– melting of the pattern material from the ceramic shell, followed by its firing and pouring of molten metal.

A significant problem is the negative impact of thermophysical phenomena, which result in changes in material volume due to thermal expansion or shrinkage. These phenomena accompany many of the technological operations mentioned above. Combatting shrinkage defects, characteristic of IC processes, which manifest both in the alloy of the casting body [13; 14] and during the production of wax models [15; 16], presents several technological challenges. The solution primarily involves ensuring a narrow pouring temperature range and controlling the solidification conditions of both the molten metal and the model mass.

For instance, during the cooling phase of the wax mass in the formation of the wax pattern, volumetric shrinkage can reach 14 %, manifesting on the surface in the form of sink marks, wrinkles, and waviness, requiring additional resources to correct these defects [17]. Preventing such defects is only partially achieved by optimizing processes at the design stage, strictly controlling the injection temperature of the pattern materials, and improving their compositions, which helps reduce the thermal expansion coefficient [18 – 21]. Geometrical distortion in castings can also occur due to the poor wettability of the wax model surface by the materials forming the ceramic shell [22]. The thermal expansion of the pattern material during its melting from the shell is also a cause of shell integrity violations [23]. The issue of low crack resistance in ceramics is sometimes addressed by reinforcing them with various materials and inserts [24]. After achieving the required ceramic thickness, shell molds are often subjected to a de-waxing process, typically performed by autoclaving. This operation also carries certain risks of damage to the inner layers due to the thermal expansion of the pattern material, which penetrates the pores of the ceramic during melting [25]. Residual wax material in the ceramic layers can affect the structure and sur-

face properties of the casting. These issues necessitate increased allowances for mechanical processing, leading to higher metal consumption.

The researchers from the Laboratory of Problems of Creation and Processing of Materials and Products at the Khabarovsk Federal Research Center of the Far Eastern Branch of the Russian Academy of Sciences have proposed a comprehensive solution to the aforementioned problems related to the thermal expansion of pattern materials. The solution involves forming wax patterns either entirely or their surface (in the case of producing wax patterns for bimetallic castings, where the surface is formed by pressing pattern material powder onto a steel frame) through cold pressing of fractions of waxy pattern materials. This approach allows for the creation of a pressed structure with porosity of up to 12 %, with the outer surface configuration corresponding to the shaping cavity of the mold [26; 27].

This method of forming wax patterns ensures that the pattern material penetrates complex shaping cavities of the press matrix and achieves the required density in sections of the compact [28; 29]. Pressed wax patterns are distinguished by the absence of such casting defects as shrinkage, waviness, or geometric distortion. During the stage of model removal from the ceramic mold, these models do not deform the shell, and the pattern material does not penetrate its structure, thereby ensuring its crack resistance. The absence of pattern material in the pores of the ceramic ensures predictable structure and surface properties of the final casting.

A drawback of the presented process is the potential for dimensional changes in the compact due to the unloading of the pattern material and the release of air trapped during compaction. The magnitude of the elastic response of the compacted material after the load is removed can reach 0.7 – 1.2 % in the pressing axis direction and 0.4 – 0.5 % in the transverse direction, which, although significantly lower than the values of volumetric shrinkage, still requires a special approach to eliminate this phenomenon [30]. The mechanical strength of porous pressed wax patterns is lower than that of traditional models but is compensated by higher thermal stability.

The magnitude of the elastic unloading of the compacted material largely depends on its rheological characteristics: elasticity, plasticity, strength, viscosity, etc. During the compaction of a plastic powder body without external heat sources, the temperature in local sections of the compact material increases. Thus, reducing the values of elastic unloading depends on both the compaction speed and the stress relaxation time [31; 32]. In view of the aforementioned, the production of pressed wax patterns or their elements with predictable dimensions and minimal geometric distortions relative to the press mold cavity appears to be a relevant task in the pressing of waxy pattern material powders.

In previous works [33; 34], various solutions were proposed for addressing the issues related to the pressing modes that ensure stress relaxation in the compacts, and consequently, a reduction in the elastic after-effect of the compacted material. However, the comprehensive study of the influence of compaction speed modes of waxy powder materials in a closed press mold on the stress-strain state of the compacts, as well as the final strength and nature of their failure, is presented here for the first time.

Thus, the purpose of the present work is to determine the influence of the movement speed of the press punch during the deformation of powder bodies composed of waxy pattern materials on the stress-strain state of the compacts formed in a closed matrix.

To achieve this goal, the following tasks were addressed in the study:

– experimental determination of the stress dependencies accompanying the stages of compaction and unloading of compacts with porosity ranging from 0 to 10 %, as a function of time, at various press punch movement rates and fractions of waxy powder materials;

– experimental determination of the ultimate compression strength as a function of the porosity of samples formed from fractions of waxy powder materials at various press punch movement rates, and evaluation of the influence of pressing conditions on the nature of compact failure.

Methods for conducting the study

In the experimental part of the study, which involved forming the compacts and recording stresses during their compaction and failure, the reliability of the measured stress values was ensured by using the Shimadzu AG-X Plus testing machine. The specified characteristics of this machine, as regulated by the manufacturer, include a permissible deviation of 0.03 % at a load of 100 kN and a deformation of 10 mm. Fig. 1 shows the working area of the testing machine, located between the stationary lower support *1*, which holds the press matrix *2* (fitted with a punch), and the moving rod *3*. The press matrix is made of steel grade 45 in the form of a hollow blind-bottom cylinder with an inner diameter of $d = 44$ mm and a wall thickness of 4 mm, which, within the scope of this experiment, allows it to be considered non-deformable. The mold cavity was filled with a calculated dose of waxy powder material required for each experiment. For the experimental tasks, waxy powders commonly used in investment casting processes, corresponding to the first classification group of model compositions, were employed [6]:

– refined paraffin of grade T1, with a melting point of 60 °C and a density of $\rho_{T1} = 0.86$ g/cm^3 in the cast state;

– PS50/50 (a paraffin-stearin alloy in a 1:1 ratio), with a melting point of 52 °C and a density of $\rho_{PS50/50} = 0.935$ g/cm^3 in the cast state.

The melting point and density of the materials in their cast state are essential for ensuring the accuracy of the experimental data. These values slightly differ from the characteristics specified by relevant GOST standards (for example, "Petroleum solid paraffins. Specifications. GOST 23683–89") and were determined experimentally. The melting points of T1 and PS50/50 were preliminarily determined using the Shimadzu DTG-60H differential thermal analyzer during the heating of these materials at a rate of 2 °C/min [17]. Since the materials used in the study are low-melting, the experiments were conducted at ambient temperatures of 20 ± 2 °C. The powder fractions of the waxy materials mentioned above were obtained by sieving through model 026 sieves in the technologically preferred standard size range of 0.63 to 2.5 mm [33]. Using smaller fractions is impractical due to the high tendency of the material to cake, and using fractions larger than 2.5 mm may, in some cases, lead to the formation of "arches" in the inner sections of complex-shaped molds, causing uneven material distribution and, as a result, compacts with zones of local over-compaction. The bulk density values (ρ_{bulk}) depend on the type and fraction of the materials and are as follows: for T1 with a fraction of 2.5 mm, $\rho_{bulk} = 0.360$ g/cm^3; for T1 with a fraction of 0.63 mm, $\rho_{bulk} = 0.320$ g/cm^3; for PS50/50 with a fraction of 2.5 mm, $\rho_{bulk} = 0.340$ g/cm^3; and for PS50/50 with a fraction of 0.63 mm, $\rho_{bulk} = 0.310$ g/cm^3.

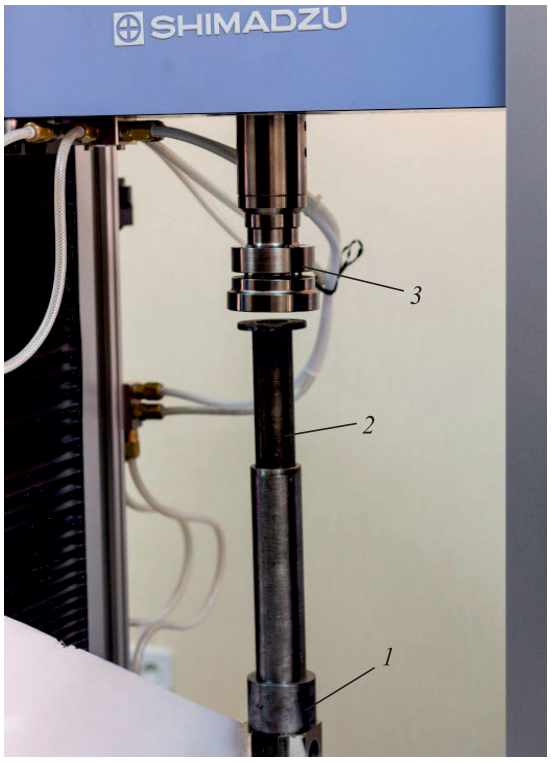

Fig. 1. Press matrix and working area of the testing machine

Рис. 1. Пресс-матрица и рабочая зона тестовой машины

To reduce the effect of friction between the material and the inner surface of the press mold on the stress values that occur during compaction, the mold cavity was treated with kerosene. The uniform distribution of the material within the volume of the powder body placed in the press mold was achieved by pre-vibrating it for 5 min at a frequency of 3.5 Hz. After the vibration process, the experimental materials were compacted at press punch movement speeds of 0.5 mm/s and 1.5 mm/s, which were controlled by the movement of the crosshead of the universal testing machine AG-X Plus Shimadzu. As a result of the uniaxial movement of the punch, a compact was formed in the lower part of the press mold, with final dimensions satisfying the condition: $d = h = 0.44$ m (where h is the final height of the compact).

The dose of waxy powder material was determined by the final porosity of the compacts, which in the experiment varied in increments of 2 % within the range 0 % ≤ P ≤ 10 %, depending on the mechanical characteristics of the compacts. For example, in preliminary experiments, it was found that compacts with porosity P > 10 % exhibited reduced strength.

The porosity of the compact was calculated using the formula

$$P = \left(1 - \frac{\rho_p}{\rho_c}\right) 100\ \%, \qquad (1)$$

where ρ_p is the density of the compact, kg/m^3, and ρ_c is the density of the cast material, kg/m^3.

It is evident that compacts with a porosity of P = 0 % will have a density equal to the density of the material in its freely cast state, which for materials of grades T1 and PS50/50 $\rho_{cT1} = 0.86$ g/cm^3 and $\rho_{cPS50/50} = 0.935$ g/cm^3.

The mass M of the waxy powder material required to form a compact with the desired porosity was determined based on the condition

$$M = h\rho_c \left(1 - \frac{P}{100}\right)\left(\frac{\pi d^2}{4}\right). \qquad (2)$$

The Table presents the values of the mass and bulk density of the powdered materials of grades T1 and PS50/50 used in the experiment to form compacts with final porosity in the range of 0 % ≤ P ≤ 10 %.

From the data presented in the Table, it is evident that the values of the final porosity of the compacts, in this case confined within the volume of a cylindrical cavity with a diameter and height of 44 mm, determine the mass and bulk

Values of masses and bulk density of waxy materials powders

Значения масс и насыпной плотности порошков воскообразных материалов

Porosity, %	Filling mass, g / Bulk density, g/cm^3	
	T1	ПС 50/50
0	57.51/0.8600	62.52/0.9350
2	56.36/0.8428	61.27/0.9163
4	55.21/0.8256	60.02/0.8976
6	54.06/0.8084	58.77/0.8789
8	52.91/0.7912	57.52/0.8602
10	51.76/0.7740	56.27/0.8415

density values of the powdered materials used in the experiment. These factors, combined with the material fractions, account for the varying heights of the powder filling in the shaping cavity of the press matrix and, consequently, the differences in the deformation values of the compacted powder bodies. Thus, it is clear that at equal press punch movement rates, the time required to obtain compacts with different final porosity values will vary.

Fig. 2 presents the experimental dependencies of the deformation of powder bodies composed of T1 and PS50/50 materials with fractions of 0.63 and 2.5 mm, as a function of the compaction time to achieve porosity values of 0 % ≤ P ≤ 10 %, with press punch movement rates of 1.5 mm/s (*a*) and 0.5 mm/s (*b*). These dependencies are shown in different colors. The equations corresponding to each curve are displayed in the same color scheme on the graph. For each curve shown in Fig. 2, the porosity values decrease from 10 to 0 % as the compaction time increases (i.e., from left to right).

It can be seen from Fig. 2 that the deformation magnitude of the compacted powder bodies for compacts with all porosity values does not exceed 60 %. Additionally, larger fractions of homogeneous materials exhibit higher bulk density values and, consequently, slightly lower final deformation values.

Once the height *h* was reached, the crosshead of the testing machine was fixed, and the stresses were recorded. One of the factors affecting the geometry of the resulting porous wax patterns is the magnitude of residual stresses in the compact material. Therefore, after the compaction process was completed, the samples were held under load with the press mold elements closed for 15 min. Preliminary experiments established that this amount of time is sufficient for stress relaxation to 90 % or more [33].

Next, to determine the maximum stresses corresponding to the failure of the samples and the nature of their

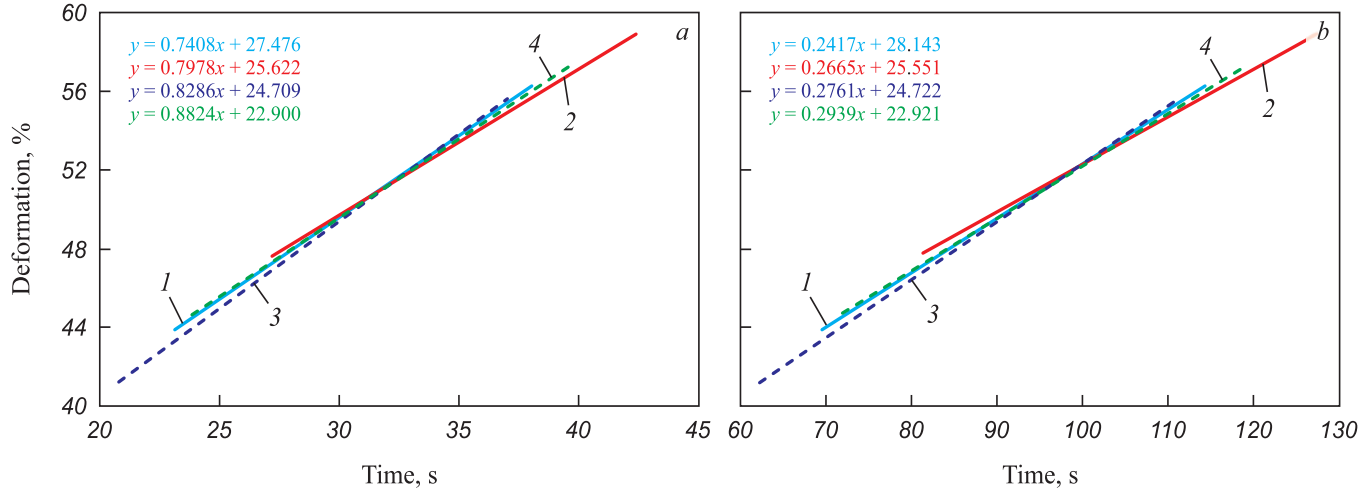

Fig. 2. Dependence of powder body deformation on time of its compaction when moving the press punch at a rate of 1.5 mm/s (*a*) and 0.5 mm/s (*b*):
1 – T1, fraction 0.63 mm; *2* – PS50/50, fraction 0.63 mm; *3* – T1, fraction 2.5 mm; *4* – PS50/50, fraction 2.5 mm

Рис. 2. Зависимости деформации порошкового тела от времени его уплотнения при перемещении пресс-пуансона со скоростью 1,5 мм/с (*a*) и 0,5 мм/с (*b*):
1 – Т1, фракция 0,63 мм; *2* – ПС50/50, фракция 0,63 мм; *3* – Т1, фракция 2,5 мм; *4* – ПС50/50, фракция 2,5 мм

failure, the resulting compacts were subjected to a compression test, as shown in Fig. 3.

The stresses arising during the determination of the compressive strength of the experimental cylindrical compacted samples were also recorded using the AG-X Plus Shimadzu testing machine. Since waxy powder materials are not structural materials and there are no standards for this type of testing, the movement speed of the testing machine's crosshead was selected at 22 mm/min, in accordance with GOST 4651–2014 "Plastics. Compression testing method".

Based on the data obtained from the series of experiments, the dependencies of the stresses accompanying the stages of material compaction and unloading on time, as well as the stresses arising during compression tests as a function of the porosity of the samples formed at various deformation rates, were plotted.

Results and discussion

The waxy model compositions used in the present experiment have a relatively high yield point [34], which naturally influences the nature of the compaction process of the powder body and the formation of the final properties of the compact. During the forming of materials with significant plasticity, the stages of the pressing process occur simultaneously, and the sections of the curves characterizing the compaction stages overlap with each other. Thus, in the case under consideration, the stages of the forming process in a closed press matrix (typical of the sequential stages of ideal compaction), such as structural deformation of the powder body, pressure increase without an increase in compact density, and subsequent plastic deformation distributed throughout its volume, have no clear boundaries.

Fig. 3. Placing an experimental cylindrical sample in the testing machine during a compression test

Рис. 3. Размещение экспериментального цилиндрического образца в тестовой машине при испытании на сжатие

As a result of the experiment, the stress dependencies accompanying the compaction and unloading stages of the compacts, with final porosity values of P = 0 – 10 %, were determined as a function of time, using various press punch movement speeds for fractions of waxy powder materials.

Fig. 4 shows the stress dependencies accompanying the compaction stages up to a porosity value of 0 % and the unloading stages as a function of time for compacts made from T1 and PS50/50 materials with fractions of 0.63 mm (*a*) and 2.5 mm (*b*). Fig. 5 shows similar stress dependencies for the processes of forming compacts with a porosity of P = 10 %.

The sections of the dependencies shown in Figs. 4 and 5 that lie in the region of negative time values characterize the compaction processes of waxy powder bodies.

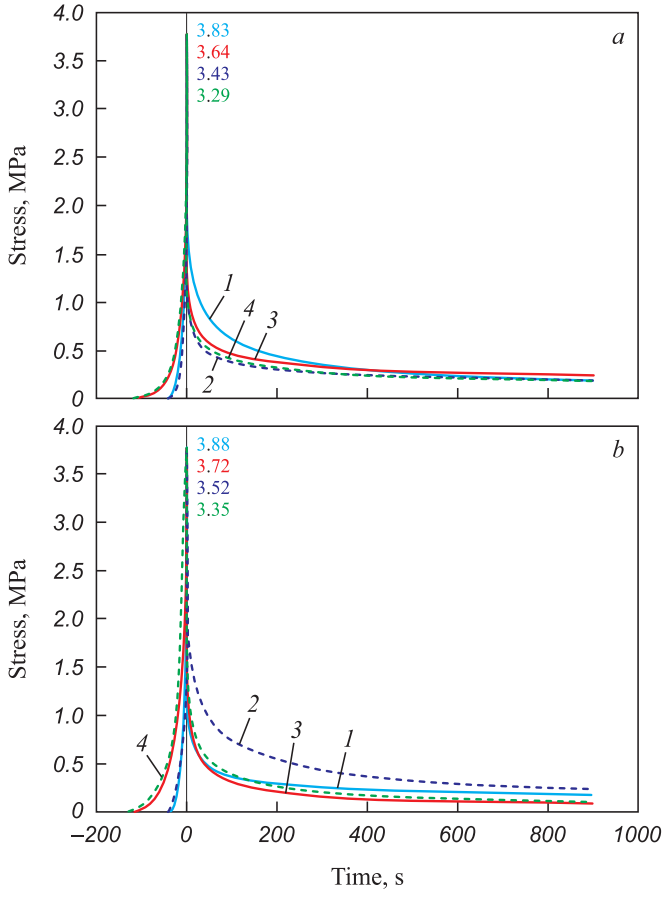

Fig. 4. Dependences of the stresses accompanying the stages of compaction to a porosity of 0 % and outloading of compacts from materials of grades T1 and PS50/50 with a fraction of 0.63 mm (*a*) and 2.5 mm (*b*) on time:
1 – T1, rate 1.5 mm/s; *2* – PS50/50, rate 1.5 mm/s;
3 – T1, rate 0.5 mm/s; *4* – PS50/50, rate 0.5 mm/s

Рис. 4. Зависимости напряжений, сопровождающих стадии уплотнения до значения пористости 0 % и разгрузки от времени прессовок из материалов марок Т1 и ПС50/50 фракций 0,63 мм (*a*) и 2,5 мм (*b*):
1 – Т1, скорость 1,5 мм/с; *2* – ПС50/50, скорость 1,5 мм/с;
3 – Т1, скорость 0,5 мм/с; *4* – ПС50/50, скорость 0,5 мм/с

The peak stress values arising during the compaction of powder bodies are indicated by numbers on the graph.

It can be seen from Fig. 4 that an increase in the press punch movement rate leads to an increase in the stress values required for forming the compacts. Moreover, the compaction of the T1 powder material is characterized by slightly higher stress values compared to the compaction of the paraffin-stearin material PS50/50, which exhibits greater plasticity. The material fraction of the pattern material (at the press punch movement rates used in this experiment) significantly influences the stress values arising during the compaction of the powder body, primarily under conditions of pressing bodies with low porosity. Thus, the largest stress values arising during the compaction of the powder bodies examined in this experiment are determined by conditions where the powder body consists of the largest fraction, compaction occurs at higher press punch movement rates, and the required final porosity value is minimal.

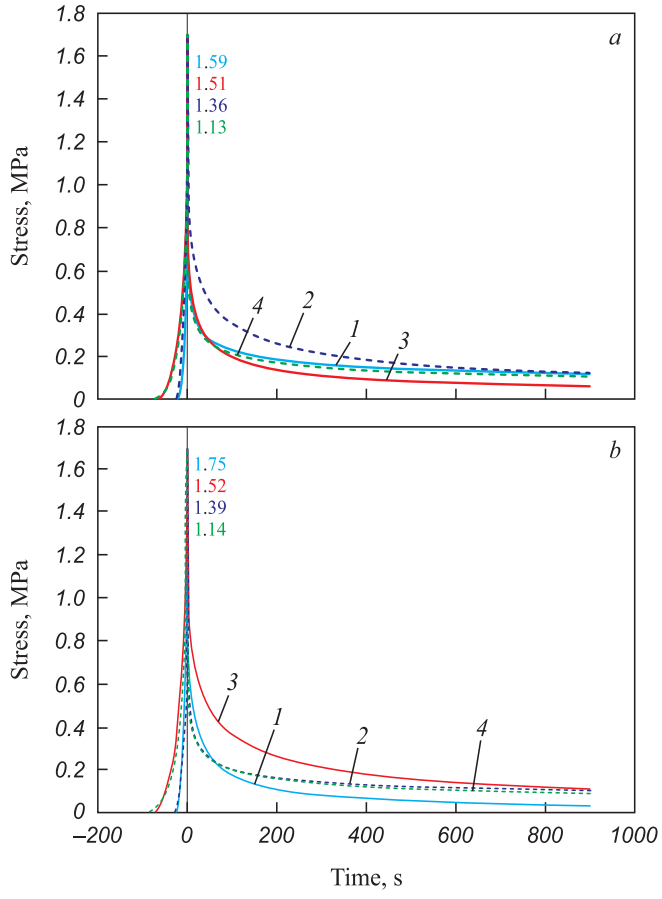

Fig. 5. Dependences of the stresses accompanying the stages of compaction to a porosity of 10 % and outloading of compacts from materials of grades T1 and PS50/50 with a fraction of 0.63 mm (*a*) and 2.5 mm (*b*) on time:
1 – T1, rate 1.5 mm/s; *2* – PS50/50, rate 1.5 mm/s;
3 – T1, rate 0.5 mm/s; *4* – PS50/50, rate 0.5 mm/s

Рис. 5. Зависимости напряжений, сопровождающих стадии уплотнения до значения пористости 10 % и разгрузки от времени прессовок, формируемых из материалов марок Т1 и ПС50/50 фракций 0,63 мм (*a*) и 2,5 мм (*b*):
1 – Т1, скорость 1,5 мм/с; *2* – ПС50/50, скорость 1,5 мм/с;
3 – Т1, скорость 0,5 мм/с; *4* – ПС50/50, скорость 0,5 мм/с

It is evident that at higher press punch movement rates, the deformation time is reduced. However, the reduction in residual stress values does not directly depend on the press punch movement rate during the compaction of the experimental powder bodies.

A combined analysis of the data presented in Figs. 4 and 5 shows that as the porosity increases to 10 %, the stresses required for compacting the compacts decrease. The changes in the stress values presented in Fig. 5, depending on the material, press punch movement rate, and powder fraction, follow a pattern similar to the dependencies shown in Fig. 4. It is also apparent that residual stress relaxation of more than 90 % is characteristic of all compaction variations after just 10 min of holding in a confined state. Overall, it should be noted that the residual stress values after 15 min of holding the compacts under load do not exceed 0.25 MPa for compacts with P = 0 % and 0.12 MPa for compacts with final porosity P = 10 %.

According to previously obtained experimental results [33], which aimed to determine the stress values arising during the failure of experimental samples as a function of their porosity, it was established that the stresses at failure are higher the lower the porosity and the larger the fraction of the material from which the compacts are formed. However, the effects of compaction speed during the production of the compacts and material fraction on compressive strength and the nature of sample failure were not addressed.

In the experiment aimed at determining the ultimate compression strength, it was necessary to establish the dependence of this parameter on the porosity of the samples formed by the deformation of powder bodies composed of fractions of the waxy materials T1 and PS50/50 at various press punch movement speeds in a fixed mold. Fig. 6 shows the third-order polynomial dependencies of the determined parameter as a function of the porosity of samples formed at various press punch movement speeds. The reliability values of the polynomial approximation of the ultimate compression strength of the samples are indicated by the symbols R_i^2.

Analysis of the data presented in Fig. 6 reveals that the stresses arising during the failure of experimental samples under compression are dependent on the maximum stress values required for compacting the samples. Thus, the higher the press punch movement rate and the larger the material fraction (with identical pre-set values of final compact porosity), the higher the stress value during pressing and, consequently, the higher the compressive strength at sample failure.

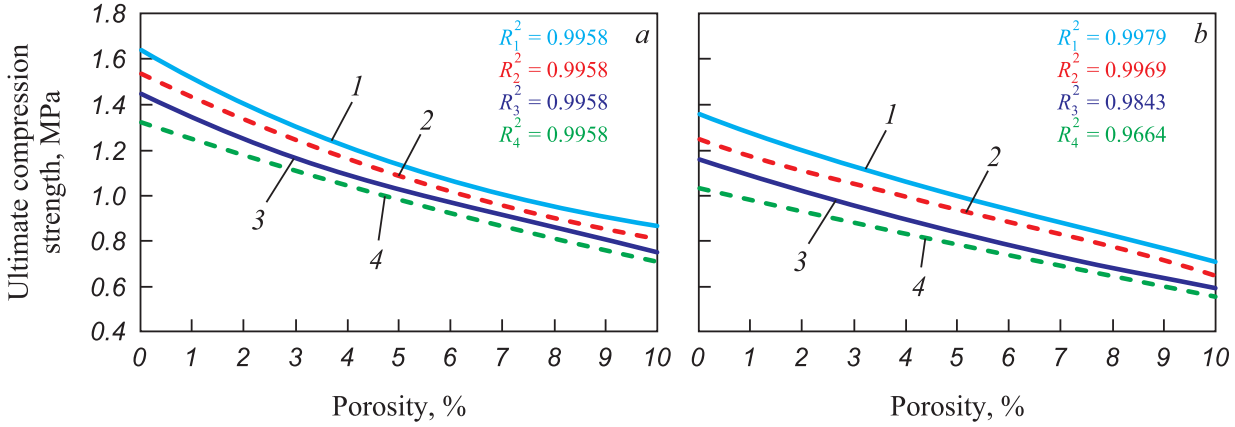

Fig. 6. Dependences of ultimate compression strength on porosity of the samples from fractions of materials of grades T1 (*a*) and PS50/50 (*b*) at different rate of press punch movement:
1 – fraction 2.5 mm, rate 1.5 mm/s; *2* – fraction 0.63 мм, rate 1.5 mm/s;
3 – fraction 2.5 mm, rate 0.5 mm/s; *4* – fraction 0.63 мм, rate 0.5 mm/s

Рис. 6. Зависимости предела прочности на сжатие от пористости образцов, сформированных из фракций материалов марок Т1 (*a*) и ПС50/50 (*b*) при различных скоростях перемещения пресс-пуансона:
1 – фракция 2,5 мм, скорость 1,5 мм/с; *2* – фракция 0,63 мм, скорость 1,5 мм/с;
3 – фракция 2,5 мм, скорость 0,5 мм/с; *4* – фракция 0,63 мм, скорость 0,5 мм/с

During the experiment, a visual assessment of the failure patterns of the experimental compacts was also conducted, and the influence of factors such as pressing speed, material fraction used in the experiment, and final compact porosity was determined. It is worth noting that, during visual observation of the compacts' deformation under compression, the material fraction and press punch movement rate during their formation had a minimal impact on the failure process. Fig. 7 shows the most typical failure patterns of compacts with minimal and maximal porosity values formed from PS50/50 material.

As shown in Fig. 7, samples with 0 % porosity typically exhibit barrel-shaped deformation under compression, indicating a more ductile type of failure. In contrast, samples with 10 % porosity tend to fail in a trapezoidal shape, with cracks forming at angles of approximately 60° to the horizontal base, suggesting a more brittle failure.

Overall, it can be concluded that while compacts made from T1 material demonstrate better resistance to compression compared to those made from PS50/50, the PS50/50 compacts still possess sufficient strength to withstand compressive loads during the application of the initial (uncured) layers of the refractory shell. The experimental data on the failure patterns of the compacts are intended to assist in determining the design, mass, and dimensions of wax patterns and/or their components produced using powder material molding techniques.

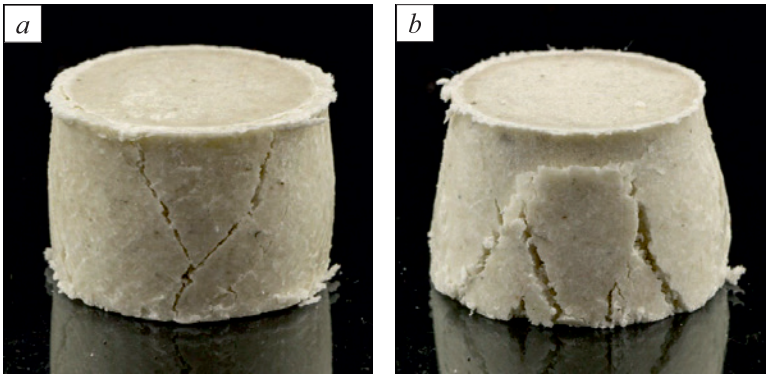

Fig.7. Nature of destruction of compacts formed at a rate of press punch movement of 0.5 mm/sec:
a – PS50/50, *P* = 0 %, fraction 0.63;
b – PS50/50, *P* = 10 %, fraction 0.63

Рис. 7. Характер разрушения образцов прессовок, сформированных при скорости перемещения пресс-пуансона 0,5 мм/с:
a – ПС50/50, П = 0 %, фракция 0,63 мм;
b – ПС50/50, П = 10 %, фракция 0,63 мм

Conclusions

As a result of a series of experiments involving the loading of waxy powder materials, holding the formed compacts in a confined state, and their failure, the influence of the press punch movement rate on the stress-strain state of the compacts formed in a closed mold was determined.

Through experimental determination of the stress dependencies accompanying the stages of compaction and unloading of compacts with a porosity of 0 – 10 % over time, at various press punch movement rates and material fractions of waxy powder materials, the following was established:

– reducing the specified values of the final compact porosity leads to an increase in the stresses arising during the compaction of waxy powder bodies and is also determined by the use of larger material fractions and compaction at higher pressing rates;

– the press punch movement rate plays a less significant role in the magnitude of the residual stresses of compacts in a confined state after compaction than the final porosity of the compacts. As a result, in the compaction of experimental powder bodies, the residual stress values after 15 min of holding the compact in a loaded state do not exceed 0.25 MPa for compacts with P = 0 % and 0.12 MPa for compacts with final porosity P = 10 %.

The analysis of the experimental data showed that increasing the press punch movement rate and increasing the fraction of the material being pressed leads to higher stress values at the failure of the experimental samples under compression. The final porosity of the compacts and the nature of the compacted material have a greater influence on whether the compacts fail in a ductile or brittle manner than the material fraction and pressing rate.

The results of this research are intended to help determine the design, mass, and dimensions of wax patterns and/or their components produced using powder material molding methods, ultimately leading to improved dimensional and geometric accuracy of the castings.

References / Список литературы

1. Wang B., Zhang Z., Xu G., Zeng X., Hu W., Matsubae K. Wrought and cast aluminum flows in China in the context of electric vehicle diffusion and automotive lightweighting. *Resources, Conservation and Recycling*. 2023;191:106877. https://doi.org/10.1016/j.resconrec.2023.106877
2. Lim S.S., Mun J.C., Kim T.W., Kang C.G. Development of low-temperature high-strength integral steel castings for offshore construction by casting process engineering. *International Journal of Naval Architecture and Ocean Engineering*. 2014;6(4):922–934. https://doi.org/10.2478/IJNAOE-2013-0222
3. Yang X., Zhang C., Li X., Cao Z., Wang P., Wang H., Liu G., Xia Z., Zhu D., Chen W.Q. Multinational dynamic steel cycle analysis reveals sequential decoupling between material use and economic growth. *Ecological Economics*. 2024;217:108092. https://doi.org/10.1016/j.ecolecon.2023.108092
4. Sata A., Ravi B. Bayesian inference-based investment-casting defect analysis system for industrial application. *International Journal of Advanced Manufacturing Technology*. 2017;90(9–12):3301–3315. https://doi.org/10.1007/s00170-016-9614-0
5. Rodriguez A., López de Lacalle L.N., Calleja A., Lamikiz A.F. Maximal reduction of steps for iron casting one-of-a-kind parts. *Journal of Cleaner Production*. 2012;24:48–55. https://doi.org/10.1016/j.jclepro.2011.11.054
6. Garanin V.F., Ivanov V.N., Kazennov S.A., etc. Investment Casting. Ozerov V.A. ed. Moscow: Mashinostroenie; 1994:448. (In Russ.).

   Гаранин В.Ф., Иванов В.Н., Казеннов С.А. и др. Литье по выплавляемым моделям. Под общ. ред. В.А. Озерова. 4-е издание, переработанное и дополненное. Москва: Машиностроение; 1994:448.
7. Dong R.Z., Wang W.H., Zhang T.R., Jiang R.S., Yang Z.N., Cui K., Wan Y.B. Ensemble learning-enabled early prediction of dimensional accuracy for complex products during investment casting. *Journal of Manufacturing Processes*. 2024;113:291–306. https://doi.org/10.1016/j.jmapro.2024.01.072
8. Pattnaik S., Karunakar D.B., Jha P.K. Developments in investment casting process – A review. *Journal of Materials Processing Technology*. 2012;212(11):2332–2348. https://doi.org/10.1016/j.jmatprotec.2012.06.003
9. Kapranos P., Carney C., Pola A., Jolly M. Advanced casting methodologies: investment casting, centrifugal casting, squeeze casting, metal spinning, and batch casting. *Reference Module in Materials Science and Materials Engineering. Comprehensive Materials Processing*. 2014;5:39–67. https://doi.org/10.1016/B978-0-08-096532-1.00539-2
10. Yarlagadda P.K.D.V., Hock T.S. Statistical analysis on accuracy of wax patterns used in investment casting process. *Journal of Materials Processing Technology*. 2003;138(1–3):75–81. https://doi.org/10.1016/S0924-0136(03)00052-9
11. Zhilin S.G., Komarov O.N., Bogdanova N.A. Production of the steel casting with improved dimensional and geometrical accuracy using complex models. *IOP Conference Series: Materials Science and Engineering*. 2020;709(3):033104. https://doi.org/10.1088/1757-899X/709/3/033104
12. Vidyarthee G., Gupta N. New development in investment casting process. *International Journal of Scientific & Engineering Research*. 2017;8(12):529–540.
13. Huang P.H., Shih L.K.L., Lin H.M., Chu C.I., Chou C.S. Novel approach to investment casting of heat-resistant steel turbine blades for aircraft engines. *The International Journal of Advanced Manufacturing Technology*. 2019;104:2911–2923. https://doi.org/10.1007/s00170-019-04178-z
14. Chen T.Y., Wang Y.C, Huang C.F., Liu Y.C., Lee S.C., Chan C.W., Fuh Y.K. Formation mechanism and improved remedy of thermal property of cold shut surface defects in Vortex Flow Meters: Numerical simulation and experimental verification in investment casting of 316 L stainless steel.

Journal of Manufacturing Processes. 2024;120:542–554. https://doi.org/10.1016/j.jmapro.2024.04.052

15. Chica E., Agudelo S., Sierra N. Lost wax casting process of the runner of a propeller turbine for small hydroelectric power plants. *Renewable Energy*. 2013;60:739–745. https://doi.org/10.1016/j.renene.2013.06.030
16. Thakre P., Chauhan A.S., Satyanarayana A., Kumar E.R., Pradyumna R. Estimation of shrinkage & distortion in Wax-Injection using Moldex3D simulation. *Materials Today: Proceedings*. 2018;5(9–3):19410–19417. https://doi.org/10.1016/j.matpr.2018.06.301
17. Zhilin S.G., Bogdanova N.A., Komarov O.N. Influence of granulometric composition and extrusion ratio of the waxy materials on the geometry of extended compact by extruding forming. *Bulletin of the Yakovlev Chuvash State Pedagogical University. Series: Mechanics of Limit State*. 2018;(4(38)): 54–64. https://doi.org/10.37972/chgpu.2020.11.35.024

    Жилин С.Г., Богданова Н.А., Комаров О.Н. Влияние гранулометрического состава и скорости выдавливания воскообразной композиции на геометрию длинномерной прессовки при мундштучном экструдировании. *Вестник Чувашского государственного педагогического университета им. И.Я. Яковлева. Серия: Механика предельного состояния*. 2018;(4(38)):54–64. https://doi.org/10.37972/chgpu.2020.11.35.024
18. Tacioglu S., Akar N. Conversion of an investment casting sprue wax to a pattern wax by chemical agents. *Materials and Manufacturing Processes*. 2003;18(5):753–768. https://doi.org/10.1081/AMP-120024973
19. Abualigah L., Abd Elaziz M., Khasawneh A.M., Alshinwan M., Ibrahim R.A., Al-qaness M.A.A., Mirjalili S., Sumari P., Gandomi A.H. Meta-heuristic optimization algorithms for solving real-world mechanical engineering design problems: A comprehensive survey, applications, comparative analysis, and results. *Neural Computing & Applications*. 2022;34:4081–4110. https://doi.org/10.1007/s00521-021-06747-4
20. Xu M., Lekakh S.N., Richards V.L. Thermal property database for investment casting shells. *International Journal of Metalcasting*. 2016;10:329–337. https://doi.org/10.1007/s40962-016-0052-4
21. Perry M.C. Investment casting. *Advanced Materials & Processes*. 2008;166(6):31–33.
22. Foggia M.D., D'Addona D.M. Identification of critical key parameters and their impact to zero-defect manufacturing in the investment casting process. *Procedia CIRP*. 2013;12: 264–269. https://doi.org/10.1016/j.procir.2013.09.046
23. Dubrovin V.K., Zaslavskaya O.M., Karpinskii A.V. Casting production from non-ferrous alloys in bulk molds of consumable patterns. *Izvestiya vuzov. Tsvetnaya metallurgiya*. 2011;(2):34–39. (In Russ.).

    Дубровин В.К., Заславская О.М., Карпинский А.В. Производство отливок из цветных сплавов в объемные формы по выплавляемым моделям. *Известия вузов. Цветная металлургия*. 2011;(2):34–39.
24. Harun Z., Kamarudin N.H., Badarulzaman N. A., Wahab M.S. Shell mould composite with rice husk. *Key Engineering Materials*. 2011;471-472:922–927. https://doi.org/10.4028/www.scientific.net/KEM.471-472.922
25. Aguilar J., Schievenbusch A., Kättlitz O. Investment casting technology for production of TiAl low pressure turbine blades – Process engineering and parameter analysis. *Intermetallics*. 2011;19(6):757–761. https://doi.org/10.1016/j.intermet.2010.11.014
26. Sosnin A.A., Bogdanova N.A., Zhilin S.G., Komarov O.N. Finite element modeling of the stress-strain state of waxy compacts. *AIP Conference Proceedings*. 2019;2176(1):030017. https://doi.org/10.1063/1.5135141
27. Bogdanova N.A., Zhilin S.G., Komarov O.N. Method for producing bimetallic casting. Patent RF 2696118, Publ. 07/31/2019. Bulletin no. 22. (In Russ.).

    Богданова Н.А., Жилин С.Г., Комаров О.Н. Способ получения биметаллической отливки. Патент на изобретение RU 2696118, опубл. 31.07.2019. Бюллетень № 22.
28. Zhilin S.G., Komarov O.N., Bogdanova N.A., Amosov O.S. Mathematical modelling of forming processes in the conditions of uniaxial compaction of powder wax-like materials. In: *CEUR Workshop Proceedings. 6 ITHPC 2021 – Short Paper Proceedings of the 6th Int. Conf. on Information Technologies and High-Performance Computing*. 2021:148–154.
29. Vinokurov G.G., Popov O.N. Statistical modeling of the correlation of local macrostructure density during one-sided pressing of powder materials. *Izvestiya Samarskogo nauchnogo tsentra RAN*. 2011;13(1–3):553–557. (In Russ.).

    Винокуров Г.Г., Попов О.Н. Статистическое моделирование корреляции локальной плотности макроструктуры при одностороннем прессовании порошковых материалов. *Известия Самарского научного центра РАН*. 2011;13(1–3):553–557.
30. Zhilin S.G., Bogdanova N.A., Komarov O.N., Sosnin A.A. Decrease in the elastic response in compacting a paraffin–stearin powder composition. *Russian Metallurgy (Metally)*. 2021;2021(4):459–463. 10.1134/S0036029521040376
31. Krairi A., Matouš K., Salvadori A. A poro-viscoplastic constitutive model for cold compacted powders at finite strains. *International Journal of Solids and Structures*. 2018;135: 289–300. https://doi.org/10.1016/j.ijsolstr.2017.11.027
32. Malkin A.Ya., Isaev A.I. Rheology. Concepts, Methods, Applications. Moscow: Professiya; 2007:560. (In Russ.).

    Малкин А.Я., Исаев А.И. Реология. Концепции, методы, приложения. Москва: Профессия; 2007:560.
33. Zhilin S.G., Bogdanova N.A., Komarov O.N. Porous wax patterns for high-precision investment casting. *Izvestiya. Non-Ferrous Metallurgy*. 2023;29(3):54–66. https://doi.org/10.17073/0021-3438-2023-3-54-66

    Жилин С.Г., Богданова Н.А., Комаров О.Н. Исследование процессов формирования пористых выплавляемых моделей, применяемых для изготовления высокоточного литья. *Известия вузов. Цветная металлургия*. 2023; 29(3):54–66. https://doi.org/10.17073/0021-3438-2023-3-54-66
34. Zhilin S.G., Bogdanova N.A., Komarov O.N. Experimental simulation of volumetric compacts formation from spherical waxy elements. *Izvestiya. Ferrous Metallurgy*. 2022;65(11):758–768. (In Russ.). https://doi.org/10.17073/0368-0797-2022-11-758-768

    Жилин С.Г., Богданова Н.А., Комаров О.Н. Экспериментальное моделирование процессов формирования объемных прессовок из сферических воскообразных элементов. *Известия вузов. Черная металлургия*. 2022;65(11):758–768. https://doi.org/10.17073/0368-0797-2022-11-758-768

Information about the Authors

Nina A. Bogdanova, *Junior Researcher of the Laboratory of Problems of Creation and Processing of Materials and Products*, Institute of Metallurgy and Mechanical Engineering of the Khabarovsk Federal Research Center, Far-Eastern Branch of the Russian Academy of Sciences
ORCID: 0000-0002-8769-8194
E-mail: joyful289@inbox.ru

Sergei G. Zhilin, *Cand. Sci. (Eng.), Assist. Prof., Leading Researcher of the Laboratory of Problems of Creation and Processing of Materials and Products*, Institute of Metallurgy and Mechanical Engineering of the Khabarovsk Federal Research Center, Far-Eastern Branch of the Russian Academy of Sciences
ORCID: 0000-0002-0865-7109
E-mail: zhilin@imim.ru

Сведения об авторах

Нина Анатольевна Богданова, *младший научный сотрудник лаборатории проблем создания и обработки материалов и изделий*, Институт машиноведения и металлургии Хабаровского Федерального исследовательского центра Дальневосточного отделения РАН
ORCID: 0000-0002-8769-8194
E-mail: joyful289@inbox.ru

Сергей Геннадьевич Жилин, *к.т.н., доцент, ведущий научный сотрудник лаборатории проблем создания и обработки материалов и изделий*, Институт машиноведения и металлургии Хабаровского Федерального исследовательского центра Дальневосточного отделения РАН
ORCID: 0000-0002-0865-7109
E-mail: zhilin@imim.ru

Received 11.07.2024
Revised 22.07.2024
Accepted 28.08.2024

Поступила в редакцию 11.07.2024
После доработки 22.07.2024
Принята к публикации 28.08.2024